JOURNAL OF SOLID STATE CHEMISTRY 83, 316–323 (1989)

Luminescence of Eu^{2+} in Strontium and Barium Thiogallates

M. R. DAVOLOS,* A. GARCIA, C. FOUASSIER,†
AND P. HAGENMULLER

Laboratoire de Chimie du Solide du CNRS, Université de Bordeaux I, 351 Cours de la Libération, 33405 Talence Cedex, France

Received February 1, 1988; in revised form August 7, 1989

Solid state investigation of the MS–Ga_2S_3 systems (M = Sr, Ba) gives evidence of the existence of the following thiogallates: $SrGa_2S_4$, $Sr_2Ga_2S_5$, $BaGa_4S_7$, $BaGa_2S_4$, $Ba_2Ga_2S_5$, $Ba_3Ga_2S_6$, $Ba_4Ga_2S_7$, and $Ba_5(GaS_4)_2$. When substituted for the alkaline earth, Eu^{2+} shows an emission in most host lattices. The emission band shifts to longer wavelengths with increasing M/Ga atomic ratio of the host lattice. For most thiogallates, despite low phonon energies and small Stokes shifts, quenching of the Eu^{2+} emission starts below 300 K. Reasons for such behaviors are discussed.

When incorporated in alkaline earth sulfides, divalent europium can show a very high luminescence efficiency. For instance, under electron beam excitation, the brightness of the red-emitting composition $Ca_{0.1}Mg_{0.9}S:Eu$ exceeds that of the Eu^{3+}-doped yttrium oxysulfide currently used in TV screens by 15% (*1*). In contrast in BaS, a host lattice whose X-ray absorption properties are quite relevant for radiology application, the Eu^{2+} emission shows poor efficiency at 300 K. Reasons for these differences have not been fully understood. Many investigations of the Eu^{2+} luminescence in MGa_2S_4 thiogallates (M: alkaline earth) have also been carried out (*2–4*). The stability of these materials toward hydrolysis is much higher than that of the binary MS sulfides and allows utilization in conventional screen-making methods. Recently several other barium thiogallates were discovered by E. Eisenmann *et al.* (*5*). By reaction of the metals or their alloys with sulfur, followed by melting, they obtained mixtures of crystals, which by structural investigations led to the compositions: $BaGa_4S_7$, $Ba_2Ga_2S_5$, $Ba_3Ga_2S_6$, $Ba_4Ga_2S_7$, and $Ba_5(GaS_4)_2$.

The variety of formulae of thiogallates makes this family quite attractive for an investigation of the parameters which govern the luminescence of Eu^{2+} in sulfides. The present paper describes the luminescence characteristics of this ion in thiogallates obtained in the SrS–Ga_2S_3 and BaS–Ga_2S_3 systems.

Experimental

Preparation

For the investigation of the MS–Ga_2S_3 systems the starting materials were alkaline earth carbonate (Merck) and gallium oxide (Touzard and Matignon, 99.999%). The

---

* Permanent address: Instituto de Quimica, UNESP, C.P. 174, 14800 Araraquara SP, Brazil.

† To whom correspondence should be addressed.

0022-4596/89 $3.00

mixture of oxides was heated 4 hr at 1000°C in a purified H_2S stream; the samples were ground and refired under similar conditions. On cooling H_2S was replaced by argon at 500°C to prevent sulfur condensation on the samples.

The doped specimens were obtained by replacing part of the alkaline earth carbonate by Eu_2O_3 (Rhone–Poulenc, 99.99%).

Optical Measurements

Diffuse reflectance spectra were recorded with a Cary 17 spectrophotometer, using MgO as a standard. Excitation and emission spectra were corrected for variation of the incident flux and detector response. Decays were obtained by excitation with a pulsed nitrogen laser ($\lambda = 337$ nm), using a boxcar averager (EGG Model 162/165).

The $SrS–Ga_2S_3$ and $BaS–Ga_2S_3$ Systems

In the $SrS–Ga_2S_3$ system, X-ray diffraction analysis showed the existence of two thiogallates: the previously known $SrGa_2S_4$ and $Sr_2Ga_2S_5$. The X-ray pattern of $Sr_2Ga_2S_5$ is similar to that of $Pb_2Ga_2S_5$ (*6, 7*) and the spectrum was indexed on the basis of an analogous orthorhombic unit cell, with space group *Pbca* and the parameters $a = 12.523 \pm 0.002$ Å; $b = 12.036 \pm 0.002$ Å; $c = 11.146 \pm 0.002$ Å. The interplanar spacings are listed in Table I.

In the $BaS–Ga_2S_3$ system the six barium thiogallates previously reported were prepared.

In all thiogallates gallium is tetrahedrally coordinated. The alkaline earth cations have various environments, the coordination number going from 6 to 12 (Table II).

The thiogallate powders are nearly white. In Figs. 1 and 2 the reflectance spectra are given and compared to those of SrS, BaS, and Ga_2S_3. The absorption edge is in the ultraviolet between 300 and 340 nm, at slightly shorter wavelength than that of SrS and BaS; it is considerably displaced with respect to that of Ga_2S_3 which lies at the limit of the visible. For an atomic ratio $M/\mathrm{Ga} \geq \frac{1}{2}$ (M = Sr, Ba), λ_{edge} tends to increase with the alkaline earth concentration. Small absorption bands in the visible are probably due to defects; their intensity increases with rising preparation temperature.

TABLE I

X-RAY DIFFRACTION DATA FOR $Sr_2Ga_2S_5$

h	*k*	*l*	$d_{\mathrm{cal.}}$ (Å)	$d_{\mathrm{obs.}}$ (Å)	I/I_0
2	1	1	4.971	4.974	5
1	1	2	4.689	4.690	17
2	0	2	4.163	4.165	5
2	1	2	3.934	3.940	30
3	1	1	3.718	3.717	28
1	3	1	3.614	3.616	15
2	2	2	3.423	3.421	100
3	0	2	3.341	3.341	5
2	3	1	3.232	3.232	25
2	1	3	3.088	3.086	12
4	1	0	3.029	3.029	12
0	4	0	3.008	3.008	20
0	4	1	2.9049	2.9051	17
1	4	1	2.8298	2.8286	23
0	0	4	2.7866	2.7853	35
3	1	3	2.7044	2.7086	40
4	1	2	2.6620	2.6616	35
2	4	1	2.6351	2.6334	5
2	0	4	2.5459	2.5450	20
4	2	2	2.4858	2.4844	7
4	3	0	2.4682	2.4682	17
4	3	1	2.4098	2.4088	5
5	1	1	2.3948	2.3944	12
2	2	4	2.3447	2.3455	7
1	5	1	2.3124	2.3140	5
1	4	3	2.2986	2.2969	5
3	1	4	2.2758	2.2768	5
2	5	1	2.2025	2.2022	3
2	3	4	2.1496	2.1476	10
4	4	1	2.1294	2.1305	8
2	5	2	2.0838	2.0837	12
5	1	3	2.0466	2.0460	30
4	4	2	2.0216	2.0218	3
2	2	5	1.9829	1.9831	3
6	2	1	1.9418	1.9417	15
6	2	2	1.8590	1.8590	10
5	3	3	1.8443	1.8443	10

TABLE II

ENVIRONMENT OF THE DIVALENT CATION AND CHARACTERISTICS OF THE Eu^{2+} EMISSION AT 90 K IN SrS AND THIOGALLATES

Host lattice	Coordination number of M^{2+} for the various types of sites	Shortest M–S distance (Å) (Ref. (5))	Bottom of the $4f \rightarrow 5d$ absorption band ($cm^{-1} \times 10^{-3}$)[a]	Energy of maximum emission ($cm^{-1} \times 10^{-3}$)	Bandwidth at half-intensity ($cm^{-1} \times 10^{-3}$)
$SrGa_2S_4$	8, 8, 8		19.9	18.58	1.33
$Sr_2Ga_2S_5$	8, 8		19.3	18.08	1.60
SrS	6		17.2	16.18	1.83
$BaGa_4S_7$	12	3.40	25.2	20.74	1.70
$BaGa_2S_4$	6, 12	3.17	22.2	19.72	1.80
$Ba_2Ga_2S_5$	7, 7	3.10			
$Ba_3Ga_2S_6$	7, 8	3.11	20.2	18.58	1.43
$Ba_4Ga_2S_7$	7, 8, 8, 9	3.06	19.2	15.29	1.97
$Ba_5(GaS_4)_2$	8, 8, 10	3.00			

[a] Taken as the intersection of the straight line corresponding to the steep edge and of the baseline in the excitation spectra.

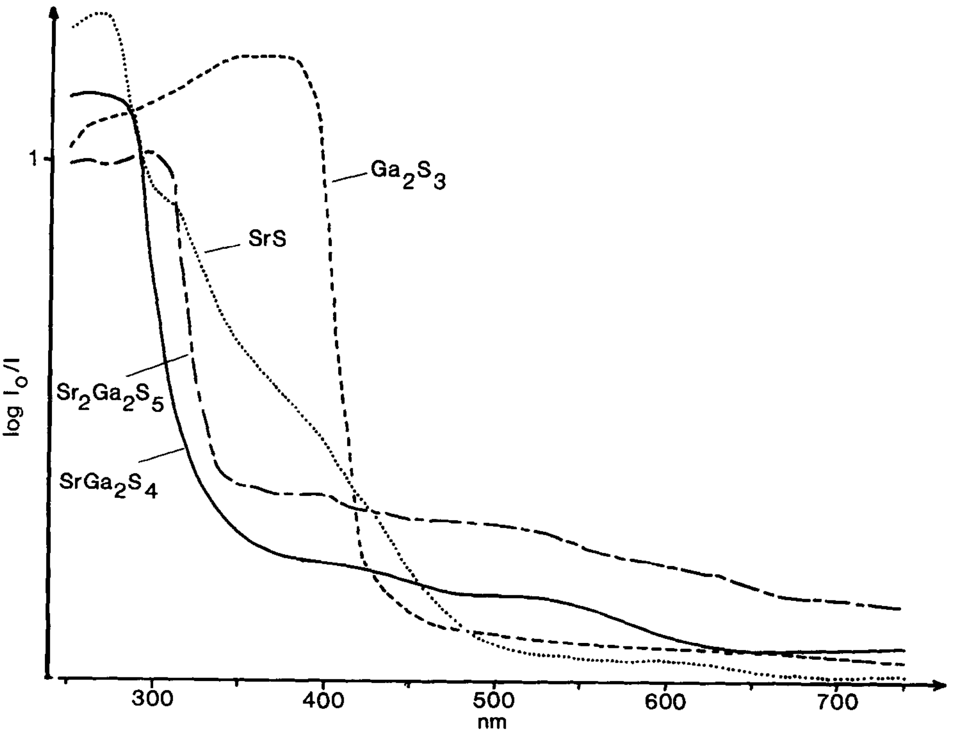

FIG. 1. Reflectance spectra of Ga_2S_3, SrS, and strontium thiogallates (T = 300 K).

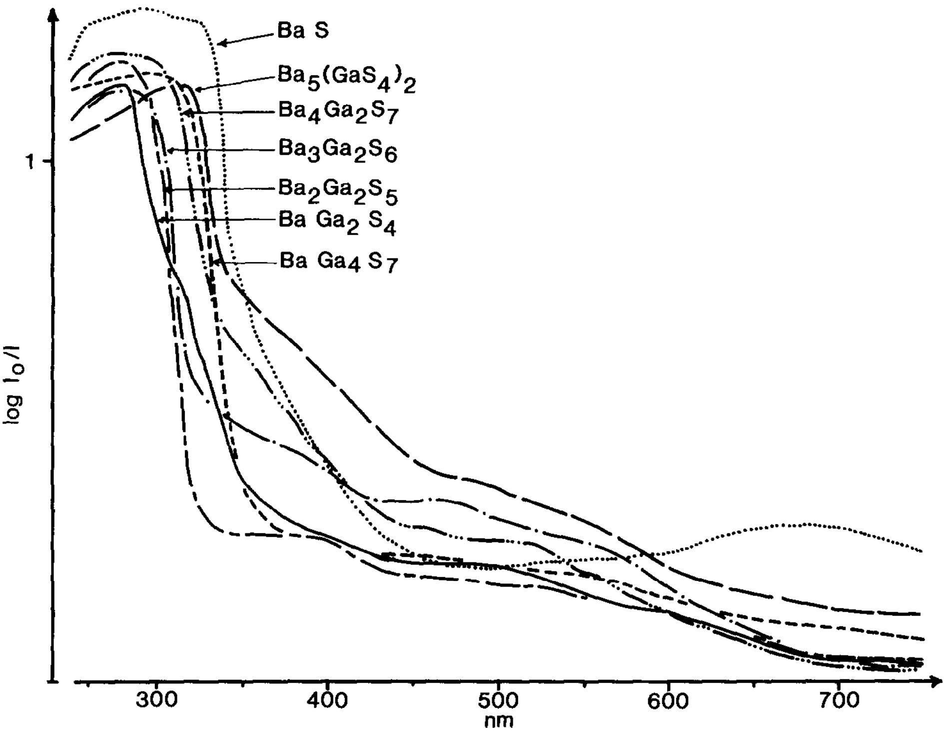

FIG. 2. Reflectance spectra of BaS and barium thiogallates.

Strontium or barium thiogallates are appropriate host lattices for divalent europium since direct $4f \rightarrow 5d$ excitation can occur, and these transitions extend to the visible in sulfides owing to the strong nephelauxetic effect (*2*, *3*).

Luminescence of Eu^{2+} in Strontium and Barium Thiogallates

Since increased absorption in the visible from rising preparation temperature is detrimental to the Eu^{2+} luminescence, the doped samples were prepared at the lowest possible temperature for complete reaction, 900 to 1000°C.

At 90 K Eu^{2+} gives an intense emission when incorporated either in $SrGa_2S_4$ and $Sr_2Ga_2S_5$ or in $BaGa_4S_7$, $BaGa_2S_4$, $Ba_3Ga_2S_6$, and $Ba_4Ga_2S_7$. Figures 3 and 4 show the luminescence spectra. No emission was detected with $Ba_2Ga_2S_5$ and $Ba_5(GaS_4)_2$ as host lattices.

The energy of the bottom of the $5d$ band derived from the excitation spectra is indicated in Table II. The $5d$ bands shift to longer wavelengths when the M/Ga ratio increases, indicating a higher ligand field at the divalent cation site or a stronger nephelauxetic effect. This result is quite consistent with the variation of the shortest Ba–S distance in barium thiogallates (Table II).

In a similar way the emission band moves to longer wavelengths. Owing to the high probability for energy transfer, the emission originates from the site generating the strongest splitting. The Stokes shift cannot be determined accurately, since the first maximum in the f–d excitation band is often difficult to identify. It ranges from about 2000–3000 cm^{-1} for $SrGa_2S_4$, $Sr_2Ga_2S_5$, and $Ba_3Ga_2S_6$ to 5000–6000 cm^{-1} for $BaGa_4S_7$,

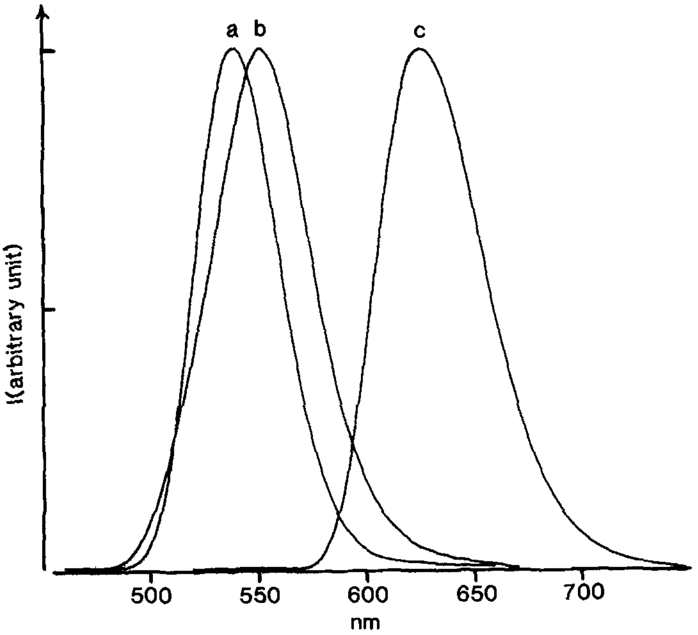

FIG. 3. Emission band of Eu^{2+} in $SrGa_2S_4$ (a), $Sr_2Ga_2S_5$ (b), and SrS (c) for excitation into the $4f \rightarrow 5d$ bands at 90 K. Fraction of alkaline earth sites occupied by Eu^{2+}: $x = 0.01$.

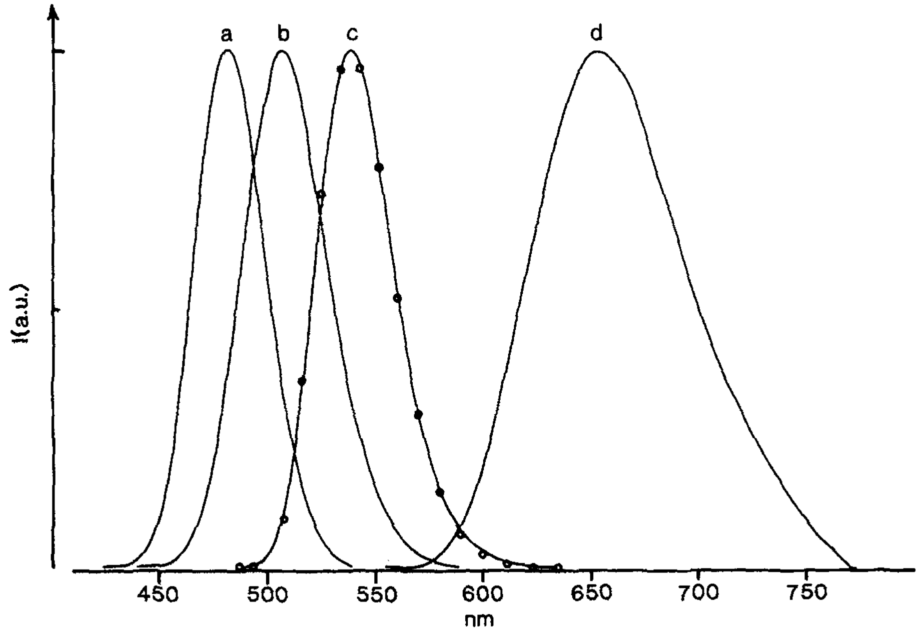

FIG. 4. Emission band of Eu^{2+} in $BaGa_4S_7$ (a), $BaGa_2S_4$ (b), $Ba_3Ga_2S_6$ (c), and $Ba_4Ga_2S_7$ (d) for excitation into the $4f \rightarrow 5d$ bands at 90 K ($x = 0.01$). The points on the $Ba_3Ga_2S_6$: Eu curve correspond to the values calculated from the configurational coordinate diagram of Fig. 7. Vibrational overlap integrals were obtained via the Manneback recursion formulae (9).

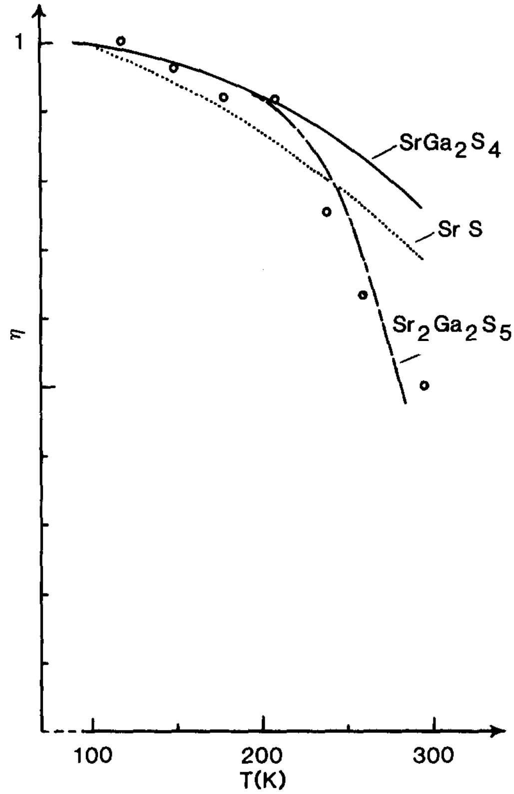

FIG. 5. Thermal behavior of the integrated emission intensity of Eu^{2+} incorporated in SrS and strontium thiogallates over the 100–300 K range ($x = 0.01$). The points represent the ratio of the decay constant at temperature T to that at low temperature for $Sr_2Ga_2S_5$: Eu.

$BaGa_2S_4$, and $Ba_4Ga_2S_7$. This variation is in agreement with that of the half-intensity width of the emission band (Table II).

Figures 5 and 6 give the temperature dependence of the emission intensity for a substitution rate x of europium for M of 1%. Quenching of the Eu^{2+} emission in the barium-rich phases, $Ba_3Ga_2S_6$ and $Ba_4Ga_2S_7$, occurs over the 100–150 K range. The intensity of $Sr_2Ga_2S_5$: Eu is reduced by half at 300 K. For other luminescent thiogallates quenching is little pronounced at room temperature and of the same order of magnitude as that of SrS : Eu (Fig. 5). As illustrated in Figs. 5 and 6 for $Sr_2Ga_2S_5$: Eu and $Ba_3Ga_2S_6$: Eu, the lifetimes of the excited states follow the same temperature dependence.

The low quenching temperature of the barium-rich phases cannot be ascribed to nonradiative $5d \rightarrow 4f$ transitions: due to the weak phonon energies in sulfides and the relatively small Stokes shift, nonradiative transitions are unable to compete with allowed radiative transitions below 300 K. The rate of nonradiative transitions is expected to increase with lowering of the $5d$ states and increasing Stokes shift (*10*). Nevertheless there is no clear correlation between these characteristics and the quenching temperature (Table II).

As an example Fig. 7 shows a single configurational coordinate diagram for Ba_3Ga_2

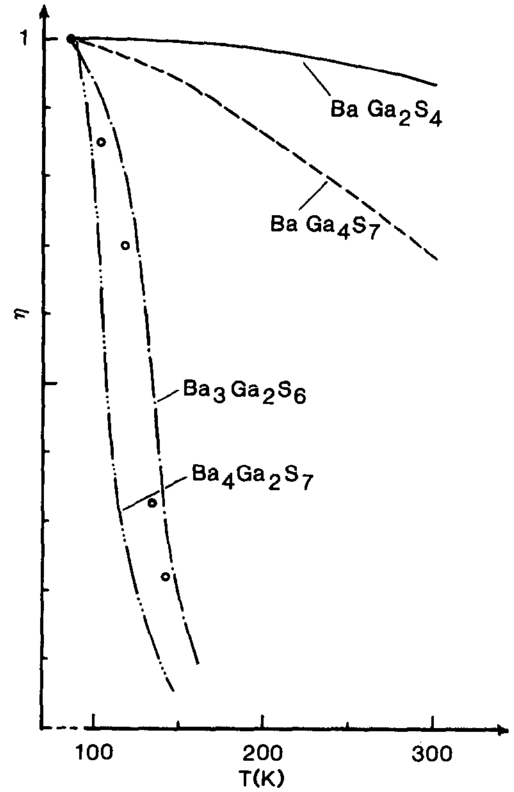

FIG. 6. Thermal behavior of the integrated emission intensity of Eu^{2+} in barium thiogallates over the 100–300 K range ($x = 0.01$). The points represent the variation of the decay constant for $Ba_3Ga_2S_6$.

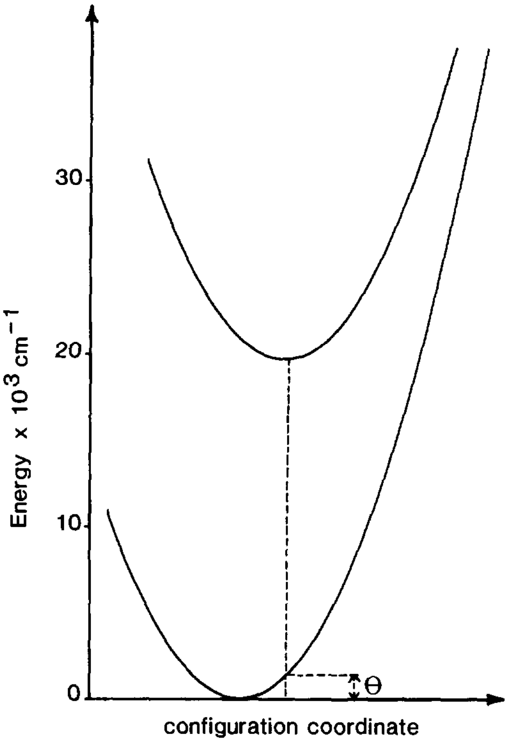

FIG. 7. Single-configurational-coordinate diagram for $Ba_3Ga_2S_6$: Eu (x = 0.01). $\hbar\omega$ = 300 cm^{-1}, and θ = 1200 cm^{-1} (offset parameter: a_{uv} = 4).

S_6 : Eu (x = 0.01). This diagram was built from the shape of the emission band and the low-energy side of the excitation band, using the quantum-mechanical model of C. W. Struck and W. H. Fonger (*8*). Best fitting was observed with phonon energies for the fundamental and excited states of about 300 cm^{-1} (a deviation is observed when the phonon energy for the excited state is chosen smaller than that of the ground state). Such a diagram predicts quenching at high temperature, well above 300 K.

The observed behavior also cannot be caused by increased energy migration among Eu^{2+} up to impurities, resulting from broadening of absorption and emission bands. If so quenching should be concentration dependent. The quenching curves obtained with samples doped with 5% Eu^{2+} were actually quite similar to those in Figs. 5 and 6.

The most probable cause for the low-temperature quenching seems to be electron transfer from the 5*d* states to the conduction band followed by nonradiative electron-hole recombination. C. Pedrini, D. S. McClure *et al.* (*11*, *12*) have shown from photoconductivity measurements that the energy difference between the ground state of divalent rare earth ions and the bottom of the conduction band in CaF_2, SrF_2, and BaF_2 decreased with increasing size of the alkaline earth. For CaF_2 and SrF_2, Eu^{2+} shows its usual $5d \rightarrow 4f$ emission, the lowest 5*d* state lying below the conduction band edge. In BaF_2 photoionization occurs, since all the 5*d* states lie above the conduction band (*13*). It can be assumed that the position of the lowest 5*d* state is close to the conduction band edge in $Ba_3Ga_2S_6$ and $Ba_4Ga_2S_7$, leading to low quenching temperatures. In $Ba_2Ga_2S_5$ and $Ba_5(GaS_4)_2$, host lattices for which no Eu^{2+} emission was detected, the level may be within the conduction band. Confirmation of the proposed mechanism would require photoconductivity measurements on single crystals. For SrS : Eu whose quenching starts below 300 K, photoconductivity does occur for irradiation in the lowest 5*d* state at room temperature (*14*).

Results obtained with thioaluminates and thiosilicates indicate similar trends (*15*). The emission of Eu^{2+} was observed in all host lattices with the exception of the barium-richest compounds, $Ba_5Al_2S_8$ and Ba_3SiS_5. Quenching temperatures are markedly higher for thioaluminates than for thiogallates. Conversely the emission of Eu^{2+} in thioindates is quenched at lower temperature (*3*). These results are consistent with the proposed interpretation since the bandgap decreases in the following order of the trivalent elements: Al > Ga > In.

Conclusions

Owing to the wide bandgap of alkaline earth thiogallates, direct excitation of the $5d \rightarrow 4f$ Eu^{2+} emission can occur. The emission band shifts to longer wavelengths with increasing M/Ga ratio. In most host lattices quenching starts below 300 K. Nonradiative losses may be the consequence of electron transfer from the excited states to the conduction band, followed by nonradiative electron-hole recombination.

Acknowledgments

The auspices of research granted by Fundaçáo de Amparo a Pasquira do Estado de Sao Paulo (FAPESP) and the travel granted by Conselho Nacional de Desenvolvimento Cientifico e Technológico (CNPQ) to M.R.D. are gratefully acknowledged. The authors are indebted to F. Guillen for technical assistance.

References

1. H. Kasano, K. Megumi, and H. Yamamoto, *J. Electrochem. Soc.* **131** (8), 1953 (1984).
2. T. E. Peters and J. A. Baglio, *J. Electrochem. Soc.* **119** (2), 230 (1972).
3. P. C. Donohue and J. E. Hanlon, *J. Electrochem. Soc.* **121** (1), 137 (1974).
4. C. Yoshida, T. Hase, and M. Shimoda, *Japan. Kokai* **77,** 124, 485; Y. Koga, W. Ichise, and T. Sumita, *Japan. Kokai* **78,** 12, 787; A. Kagami and Y. Tanigami, *Japan. Kokai* **80,** 23, 105; P. Dougier, *Eur. Pat.* **12,** 635 (1980).
5. B. Eisenmann, M. Jakowski, and H. Schäfer, *Rev. Chim. Minér.* **20,** 329 (1983); *Z. Naturforsch. b* **38,** 1581 (1983); *Rev. Chim. Minér.* **21,** 12 (1984); *Z. Naturforsch. b* **39,** 27 (1984).
6. A. Chilouet, A. Mazurier, and M. Guittard, *Mat. Res. Bull.* **14** (9), 1119 (1979).
7. A. Mazuriers, S. Jaulmes, and M. Guittard, *Acta Crystallogr. Sect. B* **36,** 1990 (1980).
8. C. W. Struck and W. H. Fonger, *J. Lumin.* **10,** 1 (1975).
9. C. Manneback, *Physica* **17,** 1001 (1951).
10. K. C. Bleijenberg and G. Blasse, *J. Solid State Chem.* **28,** 303 (1979).
11. C. Pedrini, D. S. McClure, and C. H. Anderson, *J. Chem. Phys.* **70** (11), 4959 (1979).
12. C. Pedrini, P. O. Pagost, C. Madej, and D. S. McClure, *J. Phys.* **42,** 323 (1981).
13. D. S. McClure and C. Pedrini, *Phys. Rev. B* **32** (12), 8465 (1985).
14. S. P. Keller, J. E. Mapes, and G. Cherof, *Phys. Rev.* **108** (3), 663 (1957).
15. K. Le Thi, A. Garcia, and C. Fouassier, to be published.